

Lifetime and Reorientation Measurements of 7-Azaindole and 7-Azatriptophan in Aqueous Adipic Acid Solutions: The Significance of Pendant Functionalities in Solution Phase Association Processes

L. Kelepouris and G. J. Blanchard*

Department of Chemistry, Michigan State University, East Lansing, Michigan 48824-1322

Received: March 13, 2000; In Final Form: June 13, 2000

We report on the ability of the chromophores 7-azatriptophan (7AT) and 7-azaindole (7AI) to sense aggregation of adipic acid in aqueous solution. We have studied the fluorescence lifetime and reorientation dynamics of 7AT and 7AI in water and aqueous adipic acid solutions from subsaturation through supersaturation. These probe molecules, differing by the presence (7AT) or absence (7AI) of an amino acid side group, each possess a labile proton on the chromophore ring system that renders them sensitive to changes in pH, and both chromophores are quenched collisionally in buffer solution. The dependence of the 7AI fluorescence lifetime on adipic acid concentration differs fundamentally from that of 7AT, indicating complexation of the 7AI heterocyclic nitrogen(s) with adipic acid. 7AT exhibits an increase in reorientation time near and above adipic acid saturation concentration and this trend is absent for 7AI. The 7AT amino acid side group interacts with adipic acid with a characteristic persistence time of < 50 ps. For 7AI the interaction with adipic acid is too short-lived to be seen by reorientation measurements.

Introduction

The process of crystallization from solution is of vital economic importance to many industrial processes. Crystallization is the method of choice for separation and purification in the chemical, pharmaceutical, and food industries. Controlling crystallization from solution has a direct effect on the physical properties and purity of the resulting product. To control the crystallization process, we must first understand the molecular interactions between solution constituents that can ultimately lead to crystallization. The goal of this work is to understand the role of probe molecules, which can and do act as impurities, in mediating liquid-phase self-assembly.

Crystallization from solution is a complex, dynamic process. The problems associated with studies of crystallization include determining the structure of pre-crystalline aggregates in supersaturated solutions, the nature of crystal nuclei, the influence of impurities, and the relationship between the capture of impurities and the crystallization conditions. The incorporation of impurities is perhaps the most significant matter because of the consequences and the dependence of this process on the details of intermolecular interactions in solution. For this reason we have focused on the intermolecular interactions between (fluorescent) impurity molecules and species in solution capable of crystallization.

The choice of the fluorescent probe molecules for this work is based on two criteria. First, we are interested in working with biologically benign and relevant molecules in aqueous environments because of the potential utility of such molecules to the investigation of protein and peptide structure. Second, using probe molecules with well-behaved photophysical properties allows for easier interpretation of spectroscopic data. For these reasons, tryptophan is one obvious choice. Tryptophan is an

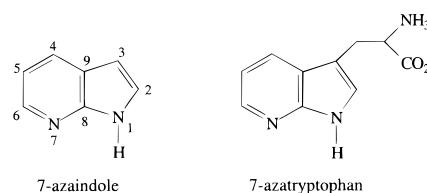


Figure 1. Structures of 7-azaindole (7AI) and 7-azatriptophan (7AT).

essential amino acid with a well-characterized fluorescence response. The fluorescence properties of tryptophan along with its chromophore moiety, indole, have been studied extensively due to its use as a standard optical probe of protein structure and dynamics.^{1–3} Unfortunately, tryptophan is characterized by nonexponential fluorescence relaxation behavior and, without the excited-state properties of the chromophore being well understood, interpreting transient fluorescence data in complex systems is problematic.^{4–6}

One consequence of this spectroscopic complication is the development of the synthetic amino acid 7-azatriptophan (7AT) and its corresponding chromophore moiety 7-azaindole (7AI) as biological probes (Figure 1).^{7–10} 7AT has been used as an alternative to tryptophan in the study of protein structure and dynamics^{8,11} because of its well-behaved, single-exponential fluorescence decay over a wide pH range.^{11,8} The 7AI chromophore is a prototypical model for excited state proton transfer, a fundamental reaction in many chemical and biochemical processes. The dimer of the 7AI chromophore is structurally similar to hydrogen-bonded DNA base pairs and is regarded as a model for the study of photoinduced mutagenesis.^{13–15}

We use these two chromophores to study the pre-crystalline aggregation behavior of aqueous adipic acid. This method is, in effect, a direct examination of impurity incorporation because it uses trace amounts of a chromophore either with (7AT) or without (7AI) a functionality in common with the crystallizing matrix. The time- and frequency-domain optical responses of

* To whom correspondence should be addressed. E-mail address: blanchard@photon.cem.msu.edu.

the probe are monitored as a function of solution composition, and these data reveal the details of the intermolecular interactions at work in these systems. The adipic acid system has been studied previously using the optical probes pyrene and pyrene carboxylic acid.¹⁶ Based on the results of that work, we expect 7AT to incorporate into adipic acid pre-crystalline aggregates through its carboxylic acid functionality. In contrast, we expect 7AI to provide the complementary, nonincorporated response. Comparing the results we report here to those for the pyrene-based probes in adipic acid solutions provides information not only on the role of different probes but also allows comparison of amino acids to carboxylic acids for their action as impurities in the crystallization of carboxylic acids.

Experimental Section

Chemicals. 7-Azaindole (99+%) and D,L-7-azatryptophan were obtained from Sigma Chemical Company and used without further purification. Adipic acid was obtained from Aldrich (99%) and used as received. The buffer solutions were made from dipotassium hydrogen phosphate and citric acid purchased from Spectrum Quality Products, Inc. All solutions were prepared with HPLC grade water from Aldrich. Solutions used for lifetime and reorientation measurements were 5 μ M in chromophore concentration. The sample cuvette was temperature-controlled with a brass block holder maintained at 20.0 \pm 0.1 $^{\circ}$ C (Neslab RTE-221).

Steady-State Absorption and Emission Spectra. Absorption spectra were acquired with a 2 nm band-pass using an ATI-Unicam double beam UV-visible absorption spectrometer. Emission spectra were recorded with one of two fluorimeters, a Hitachi F-4500 operating with 5 nm excitation and emission band-pass or a Spex 1681 Fluorolog using 2 nm band-pass for excitation and emission.

Time-Related Single Photon Counting (TCSPC) Spectrometer. The spectrometer we used for the lifetime and reorientation measurements of 7AI and 7AT has been described in detail elsewhere, and we review its salient features briefly.¹⁷ The light pulses used to excite the sample are produced with a cavity-dumped, synchronously pumped dye laser (Coherent 702-2). The dye laser is excited by the second harmonic of a cw mode locked Nd:YAG laser (Quantronix 416). Samples were excited with 290 nm light (580 nm fundamental generated using Rhodamine 6G, Kodak, SHG with KDP). Emission was monitored at the fluorescence maxima of the chromophores using a 20 nm band-pass on the collection monochromator. Fluorescence intensity decays were collected at polarizations of 0 $^{\circ}$, 54.7 $^{\circ}$ and 90 $^{\circ}$ with respect to the (vertical) polarization of the incident excitation pulse. The typical instrument response function is 35 ps and the chromophore lifetimes range from \sim 400 ps to \sim 1 ns. No deconvolution of the response function from the data was required. For the reorientation data, where $\tau_{OR} \sim$ 30–50 ps, deconvolution may be thought to be important. Analysis of the experimental data, however, show deconvolution to produce reorientation times that are the same to within the experimental uncertainty as those extracted from nondeconvoluted data.

Results and Discussion

The objective of the work we report here is to understand how each probe molecule interacts with adipic acid in aqueous solution. We are most concerned with the influence of these chromophores in the concentration region centered around adipic acid saturation. The sensitivity of these probes to their environment depends on their chemical structures and the identity of

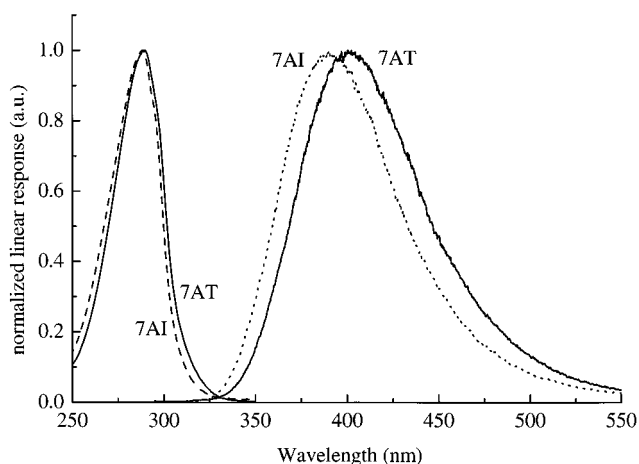


Figure 2. Linear absorption and emission spectra for the probes 7AI (dotted trace) and 7AT (solid line) in aqueous solution. Intensities of the bands have been normalized for presentation.

the solvent and saturable constituent. A prerequisite to these measurements is the development of an understanding of the probe molecule spectroscopic properties under comparatively well-controlled conditions. The steady-state linear response, fluorescence lifetime and reorientation time dependence on adipic acid concentration for both 7AI and 7AT provide the information we are interested in. We consider the steady-state optical properties of these probes first.

Steady-State Spectroscopy of 7AI and 7AT. The steady state spectroscopy of 7AI and 7AT has been investigated previously, and there is a substantial understanding of the electronic structure of these molecules. We use the information gained from this literature to aid our understanding of the data we report here. The 7AI chromophore is characterized by the presence of several electronic excited states in close energetic proximity, with the energetic spacing and transition strengths depending on the protonation condition of the heterocyclic nitrogens. At chromophore concentrations well above those we use in this work, there is some spectroscopic evidence for the formation of H-bonded oligomers.¹⁸ For the experiments we report here, we do not see evidence for H-bonded dimers that can lead to H⁺ exchange.

Linear response data provide information on the nature of the local environment sensed by the probes. Steady-state absorption and emission measurements were obtained for 7AI and 7AT in aqueous adipic acid solutions. The absorption and emission maxima of aqueous 7AI are 288 and 389 nm, respectively (Figure 2). In adipic acid solutions, the absorption band shifts to the red by \sim 2 nm, and for adipic acid concentrations higher than 10% of saturation, the fluorescence maximum of 7AI shifts to 441 nm (Figure 3a). This significant emission red shift is nearly complete by 5% of saturation and is thought to arise from protonation of the azaindole chromophore at position N₇. The ground-state pK_a of 7AI is 4.5¹⁹ and the pH for the solutions of adipic acid we use are in the range of pH 3.80 at 1% of saturation to 2.68 at 110% of saturation. A species distribution plot for 7AI (Figure 4a) indicates that the dominant species interrogated spectroscopically is the protonated form.

The sensitivity of 7AT to its local environment is similar, but more complex than that of 7AI. The presence of the amino acid side group on 7AT gives rise to a wider variety of (likely stronger) interactions with adipic acid than those seen for 7AI. The amino acid side chain of 7AT can exist in cationic, zwitterionic, and anionic forms along with the labile proton of the chromophore at N₇. Potentiometric titrations of 7AT show

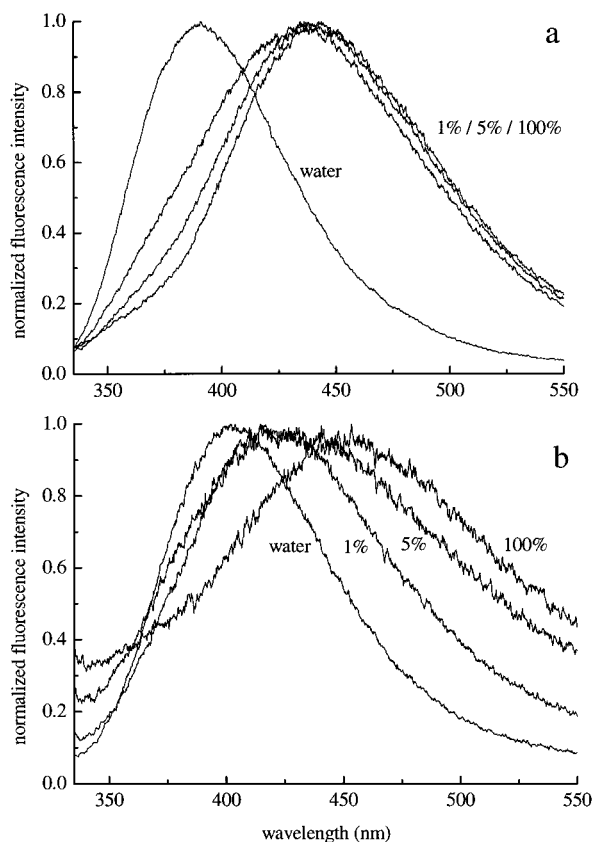


Figure 3. Normalized emission spectra for (a) 7AI and (b) 7AT as a function of adipic acid concentration. Chromophore concentrations are $5 \mu\text{M}$ for all solutions. The emission spectra shift progressively to the red with increasing adipic acid concentrations. Shown are spectra in water, 1%, 5%, and 100% of saturation adipic acid solutions.

that the ground-state pK_a values for CO_2H , N_7 , and NH_3^+ are 2.70, 3.85, and 9.35, respectively.²⁰ With these pK_a values, we calculated a species distribution plot of 7AT as a function of pH (Figure 4b). Three species coexist in the pH range of the adipic acid solutions used here. The experimental absorption maxima of 7AT aqueous and adipic acid solutions were 290 and 292 nm, respectively, showing the same behavior as we see for 7AI. The fluorescence maximum of aqueous 7AT is at 399 nm (Figure 2), and in adipic acid solutions greater than 20% of the saturation concentration the fluorescence maximum shifts to 450 nm (Figure 3b). As with 7AI, the fluorescence spectral shift with decreasing pH is the result of protonation of the azaindole chromophore at the N_7 position. The emission spectral shift is more gradual for 7AT than it is for 7AI because of the lower N_7 pK_a of 7AT (3.85) compared to that for 7AI (4.5). Because of this difference, solutions of higher adipic acid concentration are required to reach the pH values where the emission spectrum is dominated by the $\text{N}_7\text{-H}$ protonated species. For 7AT, there is also a change in the protonation of the carboxylic acid side chain in this pH range. Because the amino acid side group is not conjugated with the azaindole chromophore, we do not expect the protonation status of the amino acid carboxylic acid functionality to have a pronounced effect on the spectroscopic response of the probe.

Fluorescence Lifetimes of 7AI and 7AT. Lifetime measurements yield information on solution composition and may be sensitive to solute local organization. Due to the number of intermolecular and intramolecular factors that can influence the excited state lifetime of a given chromophore, the dependence of fluorescence lifetime on local environment remains in the

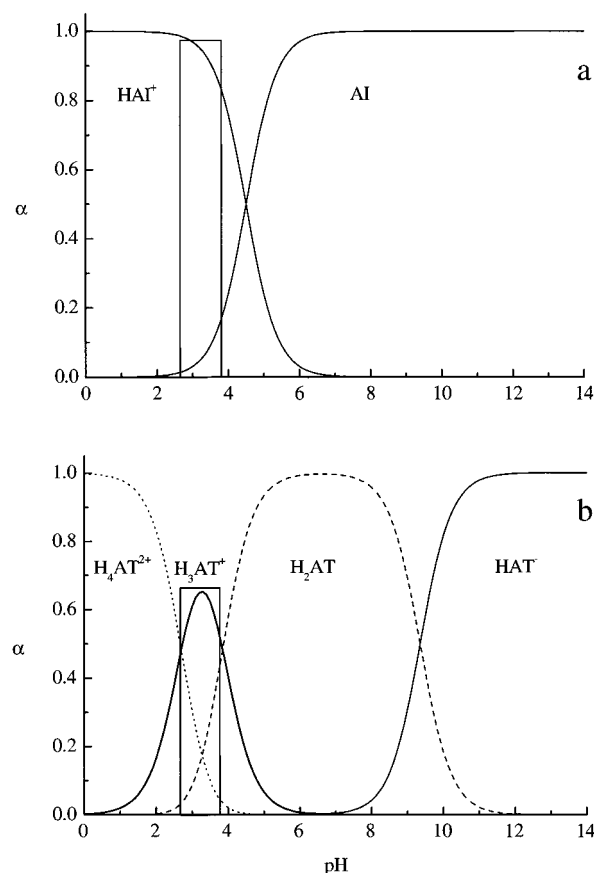


Figure 4. Calculated α -fractions for (a) 7AI and (b) 7AT. The pH range of adipic acid solutions (2.7–3.8) is boxed. The calculations were made using ground-state pK_a values for each chromophore. For 7AI, $\text{pK} = 4.5$ and for 7AT, $\text{pK}_1 = 2.70$, $\text{pK}_2 = 3.85$, and $\text{pK}_3 = 9.35$.

realm of phenomenology for most systems. For many organic molecules, the excited state lifetime depends on site-specific intermolecular interactions, such as H-bonding or complexation, and this effect can be understood in terms of the influence of the interaction on the electronic structure of the chromophore. For 7AI, the most likely locations for site-specific intermolecular interactions to occur are the $\text{N}_1\text{-H}$ and N_7 functionalities.¹⁸ The 7AI $\text{N}_1\text{-H}$ moiety will interact with its surroundings through hydrogen bonding, and there is some evidence that the strength of this interaction is related to the chromophore fluorescence lifetime.¹⁸ The relatively short lifetime (~ 900 ps) of 7AI in water at room temperature is thought to be associated with internal conversion mediated by the $\text{N}_1\text{-H}$ stretching mode or, possibly, dissociation of the N-H bond.^{19,21}

Because of the labile and environmentally sensitive nature of the N-H bond(s) in the chromophore, 7AI and 7AT are relatively sensitive to the proton content and availability of their immediate surroundings. The impact of the $\text{N}_1\text{-H}$ functionality on nonradiative decay channels is illustrated by methylation of N_1 . When N_1 is methylated, modulation of the nonradiative pathways accessed by specific interactions at the N_1 site is blocked, resulting a longer radiative lifetime. Specifically, the fluorescence lifetime of 7AT is 800 ps and that of 1-methyl-7AT is 21 ns.¹⁹

Lifetimes for 7AI were measured in aqueous adipic acid solutions over the concentration range of 0 to 110% of saturation of adipic acid. The lifetime of 7AI in aqueous solution is 912 ± 3 ps, and it increases in adipic acid solutions to ~ 1150 ps (Figure 5a). The rise in lifetime follows the adipic acid concentration dependence of the fluorescence spectral shift; it

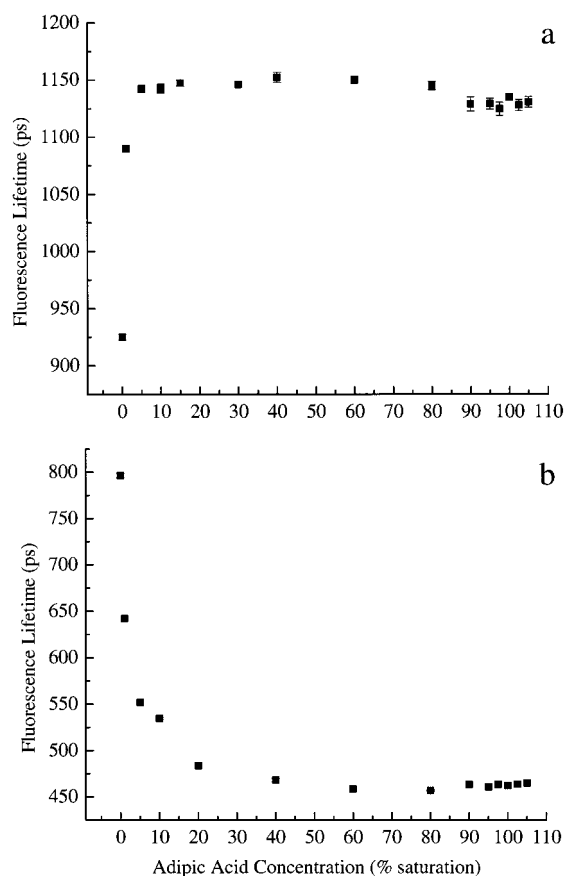


Figure 5. Fluorescence lifetimes of (a) 7AI and (b) 7AT as a function of adipic acid concentration.

is nearly complete at 1% saturation and remains constant at higher adipic acid concentrations. In principle, this lifetime change can be the result of either protonation of the chromophore at the N₇ position or complexation with adipic acid. We will return to a discussion of this point below. Under careful examination, the fluorescence lifetime of 7AI decreases slightly at higher adipic acid concentrations. This change is seen below saturation and continues through saturation. There is no indication that the fluorescence lifetime of 7AI is sensitive to any changes in local environment near saturation.

The single-exponential fluorescence lifetime of 7AT is 796 ± 3 ps in water and, in contrast to the behavior seen for 7AI, the addition of adipic acid reduces the lifetime of 7AT (Figure 5b). The change in lifetime of 7AT could also be the result of protonation of the azaindole chromophore because it follows the concentration-dependence of the steady-state fluorescence spectral shift, or it could arise from some other effect. The lifetime remains constant through saturation of adipic acid. The fact that the lifetime decreases for 7AT in adipic acid solution while that of 7AI increases under the same conditions is a clear indication that the nature of their interactions with adipic acid is different.

In an effort to elucidate the specific role of adipic acid in these measurements, we have also measured the lifetimes of 7AI and 7AT in buffer solutions. It is important to separate the adipic acid and H⁺ contributions to the lifetime dependence because we are interested in determining the role of adipic acid interactions with the chromophores. The buffer solutions spanned the same pH range as the adipic acid solutions. We used McIlvaine's buffer,²² a system consisting of citric acid and dipotassium hydrogen phosphate such that the sum of the constituent analytical concentrations is 0.1 M. The 7AI lifetime

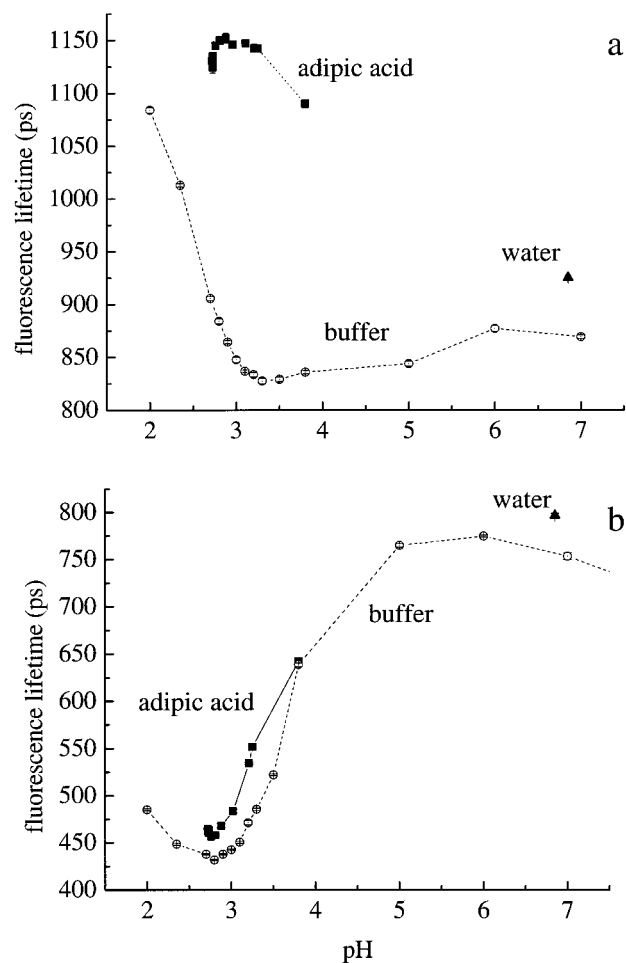


Figure 6. Fluorescence lifetimes measured for aqueous solutions containing (a) $5 \mu\text{M}$ 7AI and (b) $5 \mu\text{M}$ 7AT in adipic acid (■), buffered (○), and unbuffered (▲), aqueous solutions as a function of pH.

data are plotted for both the adipic acid the buffer solutions as a function of pH in Figure 6a. A striking feature of these data is the difference in the trends they exhibit and the large differences between lifetimes for 7AI in buffer and adipic acid solutions. For 7AT, the data, shown in Figure 6b, exhibit similar behavior for both solutions, but with an offset in lifetime at lower pH. We understand these data as follows.

The differences we observe for 7AI in buffer and adipic acid solutions cannot be based solely on pH. The direct interaction or complexation of adipic acid with 7AI must be responsible for the data shown in Figure 5a. The dependence of the 7AI lifetime on protonation at the N₇ position is manifested in the buffered solutions. The buffered solutions exhibit the same absorption and emission spectra as the adipic acid solutions at corresponding pH values, so the existence of a strong complex between adipic acid and the chromophore heterocyclic nitrogens is not evident. Thus, the formation of a weak, or short-lived complex between adipic acid and 7AI based on H-bonding interactions is likely responsible for the form of the data shown in Figure 5a. This conclusion is consistent with the reorientation data for 7AI, which we consider below.

For 7AT, the adipic acid-lifetime dependence and buffer solution pH dependence mirror one another, and these data show that the lifetime of this chromophore is determined largely by protonation at the N₇ position. If there is an interaction with adipic acid for this chromophore, it is with the amino acid side chain and not at the chromophore heterocyclic nitrogens. Again, this is an issue that can be addressed through reorientation

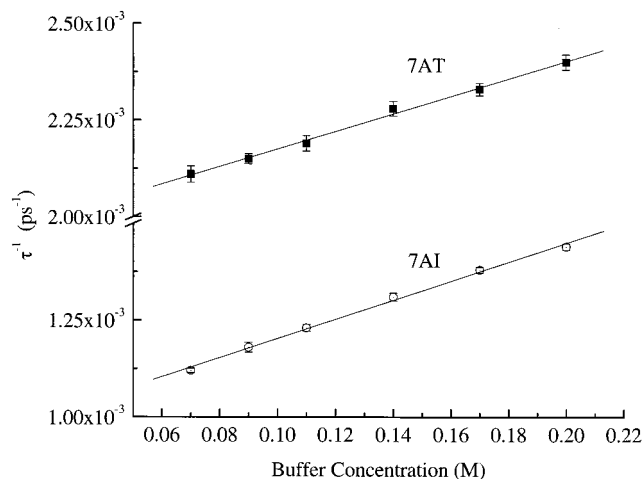


Figure 7. Stern–Volmer plots for 7AI (○, bottom trace) and 7AT (■, top trace) in citric acid/dipotassium hydrogen phosphate buffer. For 7AI $k_q = (2.5 \pm 0.1) \times 10^9 \text{ M}^{-1} \text{ s}^{-1}$ and for 7AT $k_q = (2.3 \pm 0.1) \times 10^9 \text{ M}^{-1} \text{ s}^{-1}$.

measurements (vide infra). The buffer solution pH-dependent lifetime data for 7AI and 7AT also mirror one another but are offset in pH (Figs. 6). We understand this offset as resulting from the different N_7 pK_a s for these molecules. The data in Figure 6b show a systematic offset in lifetime between the adipic acid and buffer solutions for 7AT. This offset is the result of collisional quenching interactions in the buffer solution.

There are two possible mechanisms for quenching in these systems. The first is so-called static quenching because it is mediated by the formation of a ground state complex, where only the noncomplexed species exhibits a radiative response. This type of quenching is manifested by a decrease in fluorescence intensity but with no change in fluorescence lifetime of the radiatively active chromophores. Our experimental data are not consistent with this quenching mechanism. It has been shown previously that 7AI and 7AT are quenched by KI and acrylamide,²³ and our buffer system is seen to alter the fluorescence lifetime of the chromophores. The key question here is to what extent the pH-dependent changes in lifetimes are due to $[H^+]$ and to what extent the data can be understood in terms of collisional quenching at a constant pH. We can address this issue by measuring the chromophore lifetimes as a function of buffer concentration at a constant pH.

The fluorescence lifetime of a chromophore in the presence of a collisional quencher is expected to behave according to the Stern–Volmer relationship,²⁴ given by eq 1.

$$\tau_0/\tau = 1 + K_{sv}[Q] = 1 + k_q\tau_0[Q] \quad (1)$$

where τ_0 is the lifetime of the chromophore in the absence of quencher, τ is the observed lifetime in the presence of quencher, K_{sv} is the Stern–Volmer constant, and k_q is the bimolecular quenching rate constant. Stern–Volmer plots for 7AI and 7AT in buffer solutions are shown in Figure 7. For these measurements, the total buffer concentration was varied and the pH held constant at 3.2. The Stern–Volmer plot for 7AI gives a linear fit with the slope and intercept yielding the bimolecular collision rate constant and the intrinsic fluorescence lifetime, respectively. These values, $k_q = (2.5 \pm 0.1) \times 10^9 \text{ M}^{-1} \text{ s}^{-1}$ and $\tau_0 = 1053 \pm 20 \text{ ps}$ result in a calculated value of $K_{sv} = 2.63 \text{ M}^{-1}$. The Stern–Volmer plot for 7AT yields a linear fit with $k_q = (2.3 \pm 0.1) \times 10^9 \text{ M}^{-1} \text{ s}^{-1}$, $\tau_0 = 512 \pm 6 \text{ ps}$ and $K_{sv} = 1.164 \text{ M}^{-1}$. The extrapolated values for τ_0 are in good agreement with

experiment for 7AI and are approached closely for 7AT in adipic acid at pH 3.2, where $\tau_{fl} \sim 1150 \text{ ps}$. The $\sim 10\%$ difference between the Stern–Volmer τ_0 value and the experimental τ_{fl} value in adipic acid solution is likely due to the difference in dielectric response sensed by the chromophore in the adipic acid and buffer solutions.

The Stern–Volmer plots indicate that the two probes are quenched collisionally with similar efficiency in the citric acid/dipotassium hydrogen phosphate buffer system, at least at pH 3.2. While the physics of the quenching process may be the same over the pH range of interest here, there is more than one species present for each probe at this pH, and it is possible that one form of each chromophore may be more susceptible to quenching than another. 7AI at pH 3.2 exists primarily ($\sim 95\%$) in its protonated form, and 7AT is $\sim 80\%$ protonated at the chromophore N_7 site. In addition to the issue of multiple probe molecule species being present, it is not clear from the data we report here which of the buffer constituents is responsible for the quenching. Regardless of these issues, recovery of the same value of k_q for each chromophore suggests the same quenching mechanism for each.

Reorientation of 7AI and 7AT. The steady state and fluorescence lifetime measurements provide important information regarding the local environment of the probe molecules. These data are useful but cannot, by themselves, provide a complete picture of adipic acid interactions with 7AI and 7AT in solution. To better understand the nature of the local organization present in aqueous adipic acid solutions, we have examined the rotational diffusion dynamics of 7AI and 7AT in those systems. Rotational diffusion measurements can provide information about intermolecular interactions over the length scales comparable to and greater than the dimensions of the probe molecule.^{25,26} Comparing the reorientation behavior of 7AI with that of 7AT provides direct insight into the existence and time scale of intermolecular interactions between the probe molecules and adipic acid in solution.

The theoretical framework for the interpretation of rotational diffusion data is well established,^{26,27} and both neat and binary solvent systems have been modeled effectively. Reorientation measurements sense solvent–solute interactions over a time scale in which a large number of molecular collisions occur, and the information extracted from the data is relevant to the average environment experienced by the reorienting moiety. For many binary systems, such as those reported in this work, the molecular-scale interactions responsible for the motional behavior of the probes are not modeled accurately using only the bulk solution properties and, in many cases, the results are consistent with site-specific intermolecular interactions. For polar systems, dielectric friction,²⁸ dipolar interactions,²⁹ and the formation of solvent–solute complexes³⁰ can all contribute to the reorientation behavior of a given probe molecule. We consider the reorientation behavior of 7AI and 7AT and the role that such interactions play in determining the motional properties of these probe molecules.

To obtain reorientation data, we use our TCSPC system to excite the samples with a vertically polarized light pulse and collect the time-resolved emission response at polarizations parallel ($I_{||}(t)$) and perpendicular ($I_{\perp}(t)$) to that of the excitation pulse. The combination of these time-domain data according to eq 2 yields the induced orientational anisotropy function, $R(t)$.

$$R(t) = \frac{I_{||}(t) - I_{\perp}(t)}{I_{||}(t) + 2I_{\perp}(t)} \quad (2)$$

The form of the experimental $R(t)$ function is modeled to infer

information on the chromophore local environment. The form of $R(t)$ depends on the optical properties of the probe and its interactions with its local environment. In principle, $R(t)$ can contain up to five exponential decays, depending on the angle between the excited and emitting transition dipole moments and the effective rotor shape of the probe.³¹ It is unusual to observe more than two decays in $R(t)$, and the most common case is to recover a single-exponential decay

$$R(t) = R(0) \exp(t/\tau_{\text{OR}}) \quad (3)$$

where τ_{OR} is the orientational relaxation time, related to the Cartesian components of the rotational diffusion constant, and $R(0)$ is the zero time anisotropy, related to the intrinsic spectroscopic properties of the chromophore. For the reorientation measurements we report here, $R(t)$ decays as a single exponential, as indicated in eq 3.

Extracting chemical information from reorientation data relies on relating τ_{OR} to the molecular properties of the system. The modified Debye–Stokes–Einstein (DSE) equation is the starting point for the extraction of chemical information from the decay of $R(t)$.^{32–34}

$$\tau_{\text{OR}} = \frac{\eta Vf}{k_{\text{B}}TS} \quad (4)$$

The term η is the bulk viscosity of the medium, V is the hydrodynamic volume of the probe molecule, k_{B} is the Boltzmann constant, T is temperature, S is a shape factor to account for the nonspherical shape of the probe, and f is a friction coefficient. The bulk viscosity can be measured directly, and the quantities S ³³ and V ³⁵ are determined by models and are based on the molecular structure of the probe. The term f is, effectively, the solvent–solute frictional coefficient and is estimated based on the shape of the probe.³⁴ In the stick limit, $f = 1$, and this quantity can vary from 0 to 1 in the slipping boundary condition. The values of τ_{OR} predicted by the DSE equation can be compared to those obtained experimentally as a means to gauge the strength of interaction between the probe molecule and its immediate surroundings. It is important to note, however, that there is substantial uncertainty in the determination of probe or system properties with the DSE equation. Specifically, estimation of the hydrodynamic volume, V , solute shape, S , and solvent–solute frictional term, f , all rest on model parameterizations, and the relationship between bulk and local solvent viscosity remains an open issue. Despite these limitations, comparison of experimental data to the predictions of the DSE model can provide some insight into the nature of intermolecular interactions.

Despite the simplicity of this model and the intrinsic complexity of the phenomena under consideration, the modified DSE equation provides a useful, qualitative prediction of the reorientation behavior of small molecules in polar solvents. Based on the experimental observation of a single-exponential anisotropy decay and the assumption that the dominant electronic transition is long-axis polarized,³⁶ we model 7AI as a prolate rotor. For 7AI we calculate $V = 109 \text{ \AA}^3$ using the method of van der Waals increments.³⁵ To approximate the nonspherical shape of 7AI in the context of a prolate rotor, the long-axis and short-axis molecular dimensions of the optimized geometry in the plane of the ring were used. The axial ratio was held constant and dimensions were scaled to give the calculated hydrodynamic volume. Perrin's equation³³ gives a shape factor $S = 0.82$ for a prolate ellipsoid with a major axis of 8 \AA and a minor axis of

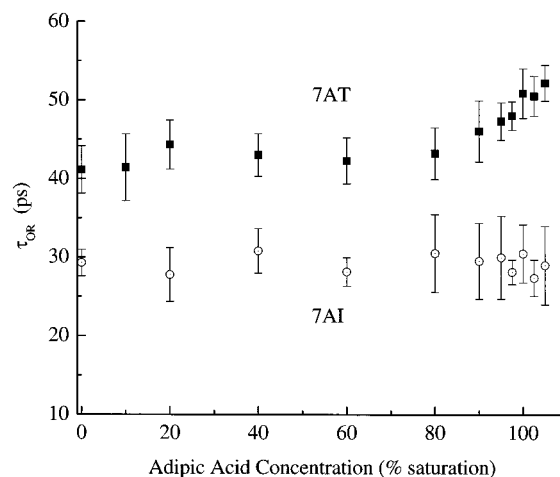


Figure 8. Reorientation data for 7AT (■, top) and 7AI (○, bottom) in aqueous adipic acid solutions.

5 \AA . Using these parameters and assuming a sticking limit boundary condition ($f = 1$), appropriate for polar solvents and solutes, we calculate a reorientation time of 32 ps for 7AI in water. This value agrees well with the experimental data for 7AI in water and in aqueous adipic acid solutions (Figure 8). The reorientation time for 7AI is constant to within experimental uncertainty for all adipic acid solutions. From our previous work we know that the bulk solution viscosity change over this range of adipic acid concentration is negligible.¹⁶ We also know from that work that, near saturation concentration, there are oligomeric adipic acid species present in solution. The reorientation data for 7AI suggest that this probe molecule does not associate strongly with the adipic acid. We do, however, know that there is a detectable interaction between 7AI and adipic acid as seen in the lifetime data (Figure 5a). The fact that we do not see any adipic acid concentration dependence to the reorientation data (Figure 8) shows that the lifetime of the 7AI adipic acid interaction is much less than the reorientation time of 30 ps.

We present our reorientation data for 7AT in Figure 8. The results for this probe molecule are qualitatively different than those we recover for 7AI. Modeling the shape of 7AT is not as straightforward as it is for 7AI. As for 7AI, the anisotropy decay is observed experimentally to be single exponential and because of the similarity of the chromophore portion of 7AI and 7AT, we model 7AT as a prolate rotor with a van der Waals volume of 179 \AA^3 .³⁵ The effective rotor shape of 7AT will not necessarily be approximated well by its optimized geometry due to the labile nature of its side chain. The one dimension that will not change is the long axis of the chromophore. We use the length of 8 \AA for this axis. The hydrodynamic volume of 7AT dictates a second axis dimension of 6.5 \AA . With these values, the shape factor S is 0.94, and modeling 7AT as a prolate rotor in the stick limit yields $\tau_{\text{OR}} = 47 \text{ ps}$. This calculated time constant falls within the range of experimental reorientation times for 7AT in aqueous adipic acid solutions (Figure 8). The adipic acid concentration dependence of the 7AT reorientation times possesses a form that is discernibly different than that seen for 7AI. The reorientation time increases from $\tau_{\text{OR}} = 43 \pm 3 \text{ ps}$ at 80% of adipic acid saturation to $\tau_{\text{OR}} = 52 \pm 2 \text{ ps}$ at 105% of saturation. This increase in reorientation time with adipic acid concentration near saturation demonstrates that 7AT senses changes in its molecular environment that are not reflected by the bulk solution. Comparing these results to those we reported previously for a different complexing system is instructive.

Previous reorientation studies of 1-pyrenecarboxylic acid in adipic acid solution led to the conclusion that adipic acid oligomers formed in solution.¹⁶ Carboxylic acids are known to form ring-bound dimers by hydrogen bonding.³⁷ For this type of complex to form, both carboxylic acid moieties must be protonated. The fact that we do not observe the same behavior for 7AT as was seen for 1-pyrenecarboxylic acid can be ascribed to the fact that the 7AT amino acid side group is largely deprotonated in the pH range we work in here. The pK_a of 1-pyrenecarboxylic acid is 4.0,³⁸ in comparison to a pK_a of 2.70 for the carboxylic acid functionality of 7AT. The experimental reorientation data do not exhibit a stepwise increase in reorientation time near saturation, as was seen for pyrenecarboxylic acid. We conclude from this finding that the details of the intermolecular interactions between 7AT and adipic acid are different than those seen between 1-pyrenecarboxylic acid and adipic acid.

The continuous trend in the reorientation time of 7AT near saturation suggests that the 7AT–adipic acid system does indeed form complexes, but the lifetime of these complexes is short relative to the reorientation time of the molecule. If we use the reorientation time of 50 ps as an estimate, at room temperature this upper bound corresponds to a complexation energy of ~ 3 – 5 kcal/mol, an energy entirely consistent with hydrogen bonding. Because this effect is seen for 7AT and not for 7AI, we infer that the interaction responsible for the behavior we observe is with the 7AT side group. There can be a number of H-bonding interactions between adipic acid and the zwitterionic amino acid group, and our experimental data do not allow resolution of this matter.

It is also possible that, near saturation, the fraction of 7AT molecules that are fully protonated increases, and such a condition could lead to stronger solvent–solute interactions, accounting for the reorientation data. The ground state α -fraction plot, shown in Figure 4b, would seem to be consistent with this possibility, but there are two factors that serve to make it unlikely. The first is that the excited-state pK_a values, which are relevant to the measurements we report here, are not known but are almost certainly quite different than those for the ground state of 7AT. The second factor that makes a change in species distribution unable to account for these data is that, in the adipic acid concentration range around saturation, there is very little change in the steady-state emission spectrum, suggesting no substantial variation in species distribution over the range where the reorientation times of 7AT vary.

Conclusions

We have examined the steady-state and time-resolved responses of 7AI and 7AT in adipic acid solutions over the subsaturation to supersaturation concentration range. Our lifetime data indicate the existence of a weak complex between 7AI and adipic acid. For 7AT, the change in lifetime with adipic acid concentration can be accounted for in terms of protonation at the N₇ position. The reorientation data for 7AT reveal interactions with adipic acid that have a characteristic persistence time somewhat less than 50 ps. The interactions seen in the 7AI lifetime data are too short-lived to be detected with reorientation measurements. The 7AT amino acid side group interacts with adipic acid in solution more strongly than do the chromophore heterocyclic nitrogens. The choice of the probe molecule for studies involving association with short-lived species can be made with reasonable certainty based on the chemical structures and properties. This work also underscores the importance of probe molecule identity and functionality

when examining multicomponent, heterogeneous systems. When this work is viewed in the context of impurity incorporation in crystallizing systems, it is clear that the chemical identity of the impurity is of central importance, consistent with the well-known structural selectivity of the crystallization process. With knowledge of the relationship between chemical structure and role in mediating crystallization, judicious choice of impurity could, in principle, be used to control crystal properties such as habit and growth rate.

Acknowledgment. We are grateful to the National Science Foundation and the Petroleum Research Fund for their support of this work.

References and Notes

- (1) Cockle, S. A.; Szabo, A. G. *Photochem. Photobiol.* **1981**, *34*, 23.
- (2) Alexander, J.; Ross, B.; Rousslang, K. W.; Brand, L. *Biochemistry* **1981**, *20*, 4361.
- (3) Chen, Lin X-Q.; Petrich, J. W.; Fleming, G. R. *Chem. Phys. Lett.* **1987**, *139*, 55.
- (4) Petrich, J. W.; Chang, M. C.; McDonald D. B.; Fleming, G. R. *J. Am. Chem. Soc.* **1983**, *105*, 3824.
- (5) Szabo, A. G.; Rayner, D. M. *J. Am. Chem. Soc.* **1980**, *102*, 554.
- (6) Robbins, R. J.; Fleming, G. R.; Beddard, G. S.; Robinson, G. W.; Thistlethwaite, P. J.; Woolfe, G. J. *J. Am. Chem. Soc.* **1980**, *102*, 6271.
- (7) Negreie, M.; Bellefeuille, S. M.; Whitham, S.; Petrich, J. W.; Thornburg, R. W. *J. Am. Chem. Soc.* **1990**, *112*, 7419.
- (8) Rich, R. L.; Negreie, M.; Li, J.; Elliott, S.; Thornburg, R. W.; Petrich, J. W.; *Photochem. Photobiol.* **1993**, *58*, 28.
- (9) Rich, R. L.; Chen, Y.; Neven, D.; Negreie, M.; Gai, F.; Petrich, J. W. *J. Phys. Chem.* **1993**, *97*, 1781.
- (10) Rich, R. L.; Smirnov, A. V.; Schwabacher, A. W.; Petrich J. W. *J. Am. Chem. Soc.* **1995**, *117*, 11850.
- (11) Hogue, C. W. V.; Szabo, A. G. *Biophys. Chem.* **1993**, *48*, 159.
- (12) Brennan, J. D.; Clark, I. D.; Hogue, C. W. V.; Ito, A. S.; Juliano, L.; Paiva, A. C. M.; Rafendran, B.; Szabo, A. G. *Appl. Spectrosc.* **1995**, *49*, 51.
- (13) Taylor, C. A.; El-Bayoumi, M. A.; Kasha, M. *Proc. Natl. Acad. Sci. U.S.A.* **1969**, *63*, 253.
- (14) Guallar, G.; Batista, V.; Miller, W. *J. Chem. Phys.* **1999**, *110*, 9922.
- (15) Fieburg, T.; Chachivili, M.; Manger, M. *J. Phys. Chem. A* **1999**, *103*, 7419.
- (16) Tulock, J. J.; Blanchard, G. J. *J. Phys. Chem. B* **1998**, *102*, 7148.
- (17) DeWitt, L.; Blanchard, G. J.; LeGoff, E.; Benz, M. E.; Liao, J. H.; Kanatazidis, M. G. *J. Am. Chem. Soc.* **1993**, *115*, 12158.
- (18) Bulska, H.; Grabowska, A.; Pakula, B.; Sepiol, J. Waluk, J.; Wild, U. P. *J. Lumin.* **1984**, *29*, 65.
- (19) Chen, Y.; Rich, R. L.; Gai, F.; Petrich, J. W. *J. Phys. Chem.* **1993**, *97*, 1770.
- (20) Chen, Y.; Gai, F.; Petrich, J. W. *J. Phys. Chem.* **1994**, *98*, 2203.
- (21) Chon, P. T.; Martinez, M. L.; Cooper, W. C.; Collins, S. T.; McMorrow, D. P.; Kasha, M. *J. Phys. Chem.* **1992**, *96*, 5203.
- (22) Day, R. A., Jr.; Underwood, A. L.; *Quantitative Analysis*, 6th ed.; Prentice Hall: Englewood Cliffs, NJ, 1991; p 155.
- (23) Petrich, R. L.; Rich, R. L.; English, D. S. *Photochem. Photobiol.* **1998**, *67*, 76.
- (24) Ingle, J. D., Jr.; Crouch, S. R. *Spectrochemical Analysis*; Prentice-Hall: Englewood Cliffs, NJ, 1988; p 343.
- (25) Jiang, Y.; Blanchard, G. J. *J. Phys. Chem.* **1994**, *98*, 9411.
- (26) Jiang, Y.; Blanchard, G. J. *J. Phys. Chem.* **1995**, *99*, 7904.
- (27) Gudgin-Templeton, E. F.; Kenny-Wallace, G. A. *J. Phys. Chem.* **1986**, *90*, 2896.
- (28) Kivelson, D.; Spears, K. G. *J. Phys. Chem.* **1985**, *89*, 1999.
- (29) Blanchard, G. J. *J. Phys. Chem.* **1989**, *93*, 4315.
- (30) Blanchard, G. J. *Anal. Chem.* **1989**, *61*, 2394.
- (31) Chuang, T. J.; Eisinger, K. B. *J. Phys. Chem.* **1972**, *57*, 5094.
- (32) Debye, P. *Polar Molecules*; Chemical Catalog Company: New York, 1929; p 84.
- (33) Perrin, F. *J. Phys. Radium.* **1934**, *5*, 497.
- (34) Hu, C. M.; Zwanzig, R. J. *J. Chem. Phys.* **1974**, *60*, 4354.
- (35) Edward, J. T. *J. Chem. Ed.* **1970**, *47*, 261.
- (36) Ilich, P. J. *Mol. Struct.* **1995**, *354*, 37.
- (37) Pauling, L.; Brockway, L. O. *Proc. Natl. Acad. Sci. U.S.A.* **1934**, *20*, 336.
- (38) Donckt, E.; Dramaix, J.; Nasielski, J.; Vogels, C. *Trans. Faraday Soc.* **1969**, *65*, 3258.